Electronic Supplementary Material (ESI) for Chemical Communications

Electronic Supplementary Information (ESI)

Intermolecular G-quadruplex-based Universal Quencher Free Molecular Beacon

Table S1. Oligonucleotides designed in the present study.

Note including abbreviation		Sequence (5'-3')
Signaling probes		
Signaling probe 8	SP8	GGGGGG**G** T(FAM) CGTTTGGTTCAAGGT CTG
Signaling probe12	SP12	GGGGGG**G** TCGTT(FAM) TGGTTCAAGGT CTG
Control signaling probe 8	CSP8	TTTTTTT T(FAM) CGTTT GGTTC AAGGT CTG
Signaling probe T	SPT	(FAM)TGGGGGG**G** TCGTTTGGTTCAAGGT CTG
Control signaling probe T	CSPT	(FAM)TAGCA CACGT ATAAA GGATC ACAC
Hemin signaling probe T	HSPT	(FAM)TGGGTAGGGCGGGTTGGG
Stretching sequences of different signaling probes		
Stretching DNA of SPT	S0	CAGACCTTGAACCAAACGACCCCCCCA
Stretching DNA of SP8	S1	CAGACCTTGAACCAAACGACCCCCCC
	S4	CAGACCTTGAACCAAACGACCCC
	S5	CAGACCTTGAACCAAACGACCC
	S7	CAGACCTTGAACCAAACGAC
	S8	CAGACCTTGAACCAAACGA
	S10	CAGACCTTGAACCAAAC
	S12	CAGACCTTGAACCAA
Stretching DNA of CSP8	C7	CAGACCTTGAACCAAACGAA
	C5	CAGACCTTGAACCAAACGAAAA
	C4	CAGACCTTGAACCAAACGAAAAA
	C1	CAGACCTTGAACCAAACGAAAAAAAA
Stretching DNA of CSPT	CT	GTGT GATCC TTTAT ACGTG TGCTA
Stretching DNA of HSPT	H1	CCCAACCCGCCCTACCCA
7C-rich sequence	7C	GAGCA CGTTT ATCCG CCCCCCCT
Oligonucleotides designed in the IGQ-MB		
Molecular beacon1	MB1	CAG ACCTT GAACC AAACG A c aacagc GGGAG AGACC GGCGCACAG gctgttg
Molecular beacon2	MB2	CAG ACCTT GAACC AAACG A c aacagc GGGAG AGACC GGCGCACAG agatctt
Molecular beacon3	MB3	CAG ACCTT GAACC AAACG A atgacac GGGAG AGACC GGCGCACAG gtgtcat
Target DNA (p53 gene)	T	CTGTGCGCCGGTCTCTCCC
Mutant target DNA	M-DNA	CTGTGCGCCAGTCTCTCCC

[a] The dye (fluorescein, FAM) is conjugated to the underlined 'T'; the base fragments with gay backgrounds denote random sequences which can hybridize with the underlined fragment in the MBs. Both the lowercase letters (called segment1) in the middle of MBs (except for MB2) and at the terminal (called segment2) can hybridize with each other to form a hairpin structure. The base in the box in segment1 is called the shared c. For MB3, there is no shared c in its segment1. Additionally, M-DNA is a mutant fragment of human p53 gene (exon8).

1. Experimental Section

1.1. Materials

All oligonucleotides (ODNs) were synthesized by Takara Biotechnology Co., Ltd. (Dalian, China) and Invitrogen Bio Inc. (Shanghai, China). They were purified by HPLC or on denaturing polyacrylamide gels. Their sequences were listed in Table S1. These DNAs were dissolved in TE buffer (10 mM Tris, 1 mM EDTA, pH 8.0) or sterile water prior to use. Exonuclease I and low molecular weight DNA ladder were purchased from New England Biolabs (Ipswich, MA). Agarose was Biowest Agarose (Spain) Products. Tris, sodium chloride and other reagents were of analytical grade and provided by China National Medicines Co. Ltd. (Beijing, China). Deionized, sterilized water (resistance >18 MΩ/cm) was used throughout the experiments.

1.2. Assay System Preparation and Fluorescence Measurements

When characterizing the fluorescence of signaling probe, a 50-μL of reaction solution containing 10 μL of signaling probe (500 nM) and 40 μL of stretching DNA at a specific concentration was allowed to incubate at room temperature for 1.5 h. Another 50-μL of dilution buffer was injected before fluorescence measurement. The final solution was kept in room temperature for another 1.5 h. Unless otherwise indicated, the concentration of ODNs is that in 50 μL of reaction solution, while the dilution and reaction buffers used in this study are buffer 1 (20 mM HEPES, 200 mM NaCl, pH 6.8). In metal ions test, 20 mM Tris buffer containing 100 mM NaCl or 50 mM $CaCl_2$ (pH 7.2) is used. Fluorescence measurements were performed using a

Hitachi F-7000 Fluorescence Spectrometer (Hitachi. Ltd., Japan). All emission spectra were collected in the range of 500 to 600 nm with an excitation and emission slit width of 5.0 nm. The excitation wavelength was 494 nm.

IGQ-MB assay system was prepared in 20-μL of binding reaction solution with 300 nM G-rich signaling probe (SP8, "8" means the fluorescein labeling at the eighth base) and 150 nM MB1 at 37 °C for 40 min. The detection was performed by adding 130 μL of target DNA sample at a specific concentration, followed by incubating at 37 °C for another 40 min. Unless otherwise indicated, the concentration of signaling probes or MB was the value obtained in a 20-μL aliquot of binding solution. The reaction buffer used in above two steps was buffer 2 (20 mM Tris-HCl, 100 mM NaCl, pH 7.2). Fluorescence measurements were carried out on a Hitachi F-4500 Fluorescence Spectrometer (Hitachi. Ltd., Japan) with the same condition as mentioned above. Fuorescence quenching ratio (Qr) was defined as:

$$Qr = \frac{F - F0}{F0} \times 100\%$$

Where F and F_0 correspond to fluorescence emission intensity observed in the presence and absence of a given target DNA concentration, respectively. The fluorescence emission intensity of SP8-based system was collected at 516 nm and CSP-based system at 520 nm. All experiments were carried out at least triplicates.

1.3. Exonuclease I Hydrolysis Assay

G-rich signaling probe samples (500 nM) were incubated in buffer 1 (20 mM HEPES, 200 mM NaCl, pH 6.8) at room temperature for 2 h. Exonuclease I (10 μL, 2

units/μL) was prepared by diluting with buffer 3 (20 mM HEPES, 200 mM NaCl, 14 mM $MgCl_2$, pH 6.8). The digestion reaction was initiated by adding exonuclease I into 10 μL of the G-rich signaling probe solution and incubated at room temperature for 2 h. Prior to fluorescence measurements, 80 μL of buffer 4 (20 mM HEPES, 200 mM NaCl, 7 mM $MgCl_2$, pH 6.8) was injected into the resulting solution. The control experiment was carried out by adding inactivate exonuclease I instead that has been boiled for 10 min.

1.4. Gel Electrophoresis

The gel electrophoresis was carried out at 120 V for 1.5 h on a 3% agarose gel with the fluorescence stain gold view in 0.5 × TBE buffer (45 mM Tris, 45 mM boric acid, 1 mM EDTA, pH 7.9) containing 20 mM NaCl. The resulting gel was visualized using a WD-9403F UV device and imaged with a Canon digital camera. Before adding loading buffer (1 μL) for electrophoresis, the sample was prepared by mixing unlabeled signaling probe (HSPT, SP8, CSP8) with stretching DNA or buffer 1 and followed by incubation at room temperature for 2 h. The final concentration of signaling probe and complementary strand are 5 μM is in the resulting mixture (20 μL). Low molecular weight DNA ladder (New England Biolabs) was used in this analysis. For IGQ-MB system, electrophoresis was performed using the DNA sample (10 μL per well) on 3% agarose gel in 1×TBE buffer (89 mM Tris, 89 mM boric acid, 2 mM EDTA, 4 mM Na^+, pH 8.0) at 100 V for 2 h. The DNA sample containing signaling probe (4 μM) and MB1 (2 μM) in reaction buffer (20 mM Tris-HCl, 100

mM NaCl, pH 7.2) was incubated at 37 °C for 80 min. The control experiments were performed by using CSP8 as signaling probe.

1.5. Circular Dichroism Spectroscopy

Circular dichroism (CD) spectra were performed on a JASCO J-820 spectropolarimeter (Tokyo, Japan) equipped with a peltier temperature controller. Three scans were accumulated and averaged under the following conditions: range from 210 nm to 350 nm, speed of 200 nm/min, response time of 0.5 s and bandwidth of 1.0 nm. All CD spectra were measured at room temperature for ODNs (5 μM) in 1 cm path length cuvette with different buffers, such as 20 mM HEPES buffer (pH 6.8) containing 200 mM NaCl and 20 mM Tris buffer (pH 7.2) containing 100 mM NaCl or 50 mM $CaCl_2$. Before the CD measurement, the DNA sample was incubated at room temperature for several hours. All ODNs used in this measurement were unlabeled DNAs.

1.6. UV Spectroscopy

UV vis absorption measurements were carried out using a MutiSpec-1501 spectrophotometer (Shimadzu, Japan) with HYPER UV Version 1.50 software. All DNA samples containing 4 μM ODNs were prepared in buffer 1 and incubated at room temperature for 3 h. The spectra were recorded at room temperature. The corresponding photo was collected under the irradiation of ultraviolet lamp.

1.7. Preparation of Hela Cell Lysate

The steps of trypsin digestion, medium washing, reaction buffer 2 (20 mM Tris-HCl , 100 mM NaCl, pH 7.2) washing and dispersion, and centrifugation were executed sequentially to obtain Hela cells. For lytic cell sample preparation, the Hela cells (~4×10^6 cells) were dipped in 2 mL of ice-cold NP-40 lysis buffer (10 mM Tris-HCl, pH 8.0; 1 mM $MgCl_2$; 1 mM EDTA; 1% (v/v) NP-40; 0.25 mM sodium deoxycholate; 10% (v/v) glycerol; 150 mM NaCl; 5 mM b-mercaptoethanol; 0.1 mM AEBSF (4-(2-Aminoethyl) benzenesulfonyl fluoride hydrochloride) for 40 min at 4°C and then centrifugated for 10 min at 10000 rpm at 4°C, then diluted to 4 mL with NP-40 lysis buffer. Finally, various amounts of target DNA were added. Before fluorescence measurements, the analysis was carried out by injecting 130 μL of lytic cell sample into 20 μL binding solution and incubating in 37 °C for 40 min.

2. Supplementary Result and Discussion

2.1. Formation of Intermolecular G-quadruplex Structure

We used four different techniques to demonstrate the real structure of our G-rich probe. First, enzymatic degradation was conducted to examine if the G-rich sequence form G-quadruplex structure. We know that exonuclease I, a single-strand specific exonuclease, degrades nucleotides from the 3' end to 5' end of linear single-stranded primer ODN[s1]. But its hydrolysis could be inhibited when the oligomer formed G-quadruplex[s2]. In this study, three signaling probes, SPT, SP8 and SP12, with covalently bound FAM at different locations of sequence (GGGGGGGTCGTTTGGTTCAAGGTCTG) (see Table S1), were synthesized to

execute digestion reaction of exonuclease I. As shown in Fig. S1 A, the fluorescence intensity of SP12 increases as the enzyme works, implying that the 3' end random fragment can be degraded. However, the fluorescence of FAM-5'-end-labeled SPT does not show any change suggesting that G_7s remains intact even if being exposed to the nuclease. This confirms the formation of G-quadruplex structures to a considerable extent. Additionally, the SP8 emission spectral intensity increases in the

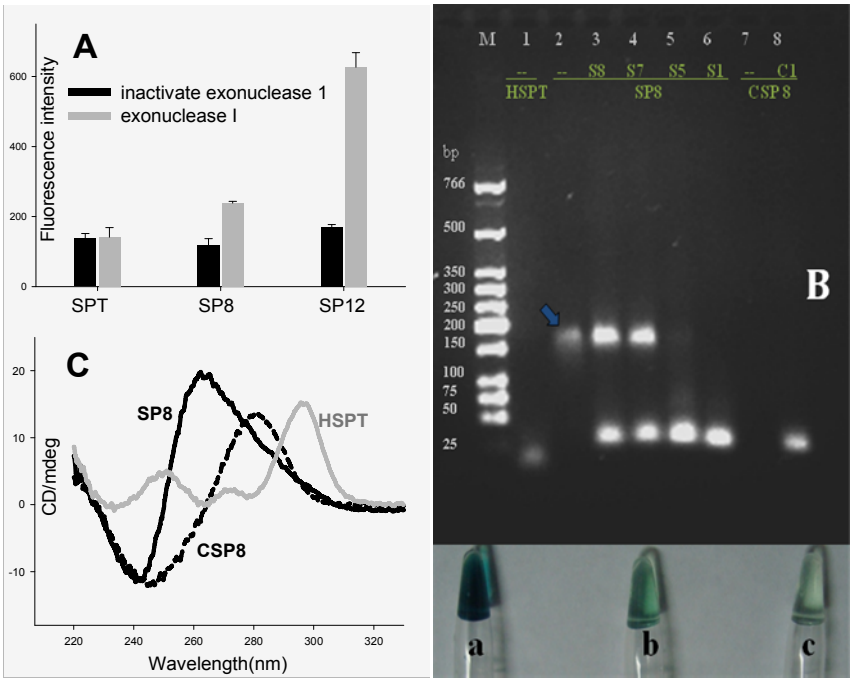

Fig. S1. (A) Response fluorescence peak of different G-rich signaling probes (SPT, SP8 and SP12 with FAM labeled at the first, 8th and 12th base of 5' end, respectively) after exposure to exonuclease I or inactivate exonuclease I. Error bars represent the standard deviation of the measurements. Spectra were recorded in buffer 1; (B) agarose gel electrophoresis image (top) showing different mobilities of three G-rich signal probes in the absence (lanes1, 2, 7) or presence (lanes 3-6, 8) of stretching sequences S8, S7, S5, S1, C1, respectively. The detailed descriptions are shown at the top of each lane. Bottom: colorimetric responses of 1 μM HSPT (a), SP8 (b) and CSPT (c) in catalytic reaction buffer (20 mM HEPES, pH 6.8, 200 mM NaCl, 0.05% (w/v) TritonX-100, 1% DMSO, 2 μM hemin, 2 mM H_2O_2, and 2 mM $ABTS^{2-}$). Photographs were taken 5 min after mixing; (C) CD spectra of ODNs SP8, CSP8 and HSPT in buffer 1. In this section, all ODNs were unlabeled and each concentration was 5 μM.

presence of exonuclease I, but the increase is not as great as that observed for SP12. It may be due to the part protection associated with the formation of G-quadruplex from the enzymatic digestion. The FAM is labeled too close to the G_7s that inhibits the hydrolysis to a certain extent. Second, another evidence for the formation of G-quadruplex structure is the measured data on the G-quadruplex-catalyzed peroxidase reaction. As already reported, hemin can intercalate into G-quadruplex structure and act as a cofactor to catalyze the oxidation of 2, 2'-azino-bis (3-ethylbenzothiazoline-6-sulfonic acid) ($ABTS^{2-}$) by H_2O_2 to the $ABTS^{-\cdot}$ colored product (green)[s3, s4]. Importantly, the activity is relative to the sequences and their kinds of G-quadruplex structures[s4]. For example, about 250-fold enhancement can be achieved when combining with G-quadruplex-based DNA aptamer of hemin than using hemin alone[s5]; besides, an obviously higher peroxidase activity will be exhibited in intramolecular structure of hemin aptamer than in intermolecular parallel-stranded G-quadruplex of $T_4G_8T_4$[s1], whereas, nearly no catalyzed peroxidase activity will be showed in a system without G-quadruplex. In this work, the visibility of green color of G-quadruplex-catalyzed peroxidase reaction is showed in Fig. S1 B (bottom) in the order: hemin aptamer (HSPT) > G-rich probe (SP8) > T-rich probe (CSP8), suggesting that SP8 with sequence of GGGGGGGTCGTTTGGTTCAAGGTCTG forms G-quadruplex structure that is different from the intramolecular type of HSPT. Third, G-quadruplex structure may be formed from one, two, four or multi-separate G-rich strands that are termed mono-, bi- and tetra- even poly- molecular G4-DNA, correspondingly[s6]. Direct evidence

showing the formation of intra- or intermolecular G-quadruplex structures was provided by using electrophoresis characterization because configuration of DNA is an important factor to affect the molecular mobility. As shown in Fig. S1 B, an obvious migration band appears in lane 1 corresponding to HSPT, while the single-stranded ODN, CSP8, exhibits no band (shown in lane 7). Due to the formation of G-quadruplex structure, the band of HSPT appears near 18 bps which is double than the real molecular weight of HSPT (18 bases), indicating intramolecular structure. Whereas, Lane 2 (SP8) has a band near 150 bps, which is about twelvefold slower than that expected, indicating that its structure is intermolecular with four or more strands binding[s7]. When stretching sequences are added, formation of SP8·strentching DNA (S8 and S7) duplex makes the band corresponding to intermolecular SP8 become lighter (lane 3 and 4), and the band of high mobility (possibly resulting from the hybridized duplexes) is also observed. The slower mobility band in lane 3 is not only significantly brighter than the faster mobility band but also enhanced by 112% in comparison to the band in lane 2. Additionally, the high mobility band is strengthened with increasing the length of stretching DNA, while the slow mobility band is weakened until disappeared in S5 and S1. This evidently suggests that S5 with three C bases more than S8 destabilizes the intermolecular structure. The experimental results showed that SP8 was mainly formed a stable intermolecular G-quadruplexes structure, though it is difficult to determine if this conformation has a tetra- or poly-molecular G4-strands in the absence of other structural data[s8]. To confirm the molecular structure of signaling probes, we further explored the topology of the structure formed

in ODNs SP8, CSP8, and HSPT by performing circular dichroism (CD) measurements (see Fig. S1C). Under the same conditions, SP8 displays a positive CD signal at near 260 nm and a negative CD signal at 240 nm characteristic of parallel conformer[s9], whereas HSPT displays a positive at around 295 and 247 nm and a negative at around 265 nm demonstrating an antiparallel G-quadruplex according to the CD data reported by Nakayam and co-workers[s3]. In comparison, CSP8 without G-runs displays a positive band at near 280 nm demonstrating a non G-quadruplex structure[s9]. On the basis of above analyses, a conclusion can be draw that the G-rich probe SP8 mainly formed intermolecular parallel G-quadruplex structure in our experiment condition (shown in Scheme 1).

2.2. FAMs Aggregation-intensified Fluorescence Quenching

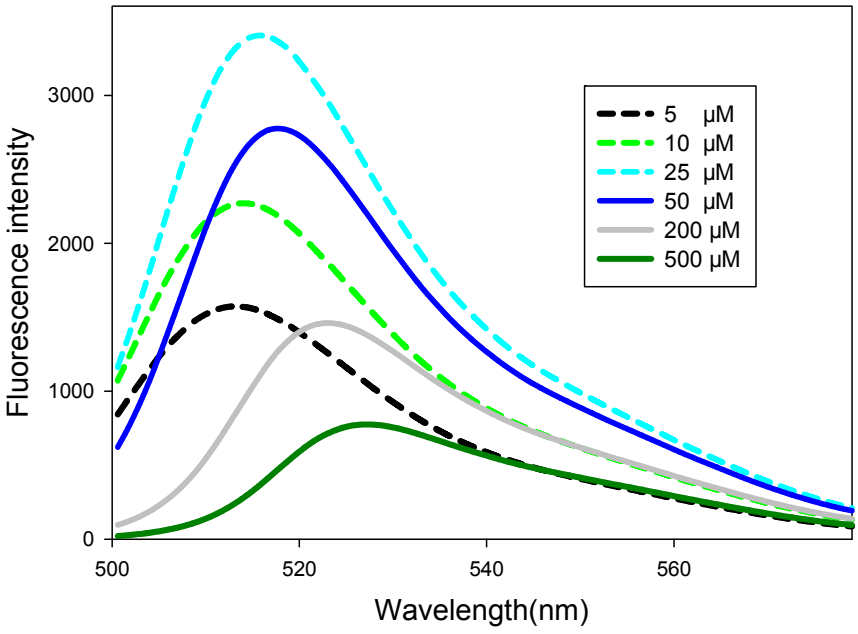

Fig. S2. Fluorescence spectra of fluorescein with various concentrations. The measurements were performed at 20 mM HEPES buffer (pH 6.8) containing 200 mM NaCl and 10% (v/v) ethanol. Ethanol promotes the dissolution of fluorescein, especially at a high concentration.

It is of great importance to explore whether the observed remarkable fluorescence quenching was triggered by the unique aggregation-induced self-quenching of FAMs or not. In the previous works,[s10] it has been advanced that concentration quenching of free fluorescein was caused by aggregation, and the fluorescence arose only from "single molecules" (monomers). The aggregation phenomena are associated with the nature of solvent and electrolytes. During analysis of the change in emission spectroscopy with increasing the concentration of fluorescein (see Fig. S2), not only a dramatic decline of spectrum intensity is observed, but also shift is detected when the concentration exceeded 25 μM. Assuming fluorescein molecule is a cube, an average distance between two dyes is 40 nm in this case. According to the literature,[s11] the quenching mechanism of 6-carboxyfluorescein (an analogous of FAM) is closely related to the dimerization and energy transfer to dimer. Moreover, Főrster critical transfer distances were calculated to be 5.1 nm and 5.7 nm for monomer-monomer and monomer-dimer transfer, respectively. In the current work, the distance between two FAMs in G-rich probe SP8 is about 1.4~3.1 nm (4~9 bases, 0.34 nm/base) whatever classical parallel or antiparallel intermolecular G-quadruplex is formed. Additionally, the UV-absorption spectra (date not shown) of oligonucleotides SP8 was lower than duplex SPT·S0, CSP8·C1 and CSP8, which is similar to the results of concentration self-quenching of dye reported by Seo[s12] and Randolph.[s13] Thus, FAMs aggregation-intensified self-quenching should happen when the signaling probes assemble into G-quadruplex structure.

2.3. Fluorescence Properties of IGQ Signaling Probe

We verified the quenching mechanisms by examining the fluorescence features of the mixtures of FAM-labeled and unlabeled G-rich sequences (counterpart strands) (shown in Fig. S3). In this experiment, ultrapure water was used to prepare signaling probe stock solution at a high concentration. Then, the sample solutions at various ratios were obtained by immediately mixing fixed volume of the signaling probe stock solution with different volume of the unlabeled counterpart strand solution, and follow by adding buffer to make the final solution (20 μL) containing 20 mM HEPES, 200 mM NaCl, (pH 6.8). In the mixtures, intermolecular G-quadruplexes are comprised of four labeled, two labeled SP8s pairing with two unlabeled counterparts or one labeled SP8 pairing with three unlabeled counterparts. That is, four FAMs, two FAMs or one FAM is involved in the corresponding G-quadruplex, where the ratios of 4:0, 2:2 and 1:3 are involved, respectively. The fluorescence increase is ~200% at the ratio of 1:3 (143 a.u.) comparing with that at 4:0 (47 a.u.). In other words, the fluorescence self-quenching efficiency of FAMs at the ratio of 4:0 is about 67%. Comparing the fluorescence value at 1:3 ratio (in this case, one FAM is involved in a G-quadruplex, and aggregation-induced self-quenching does not occur) with the CSP8 mixture (it keeps around 320 a.u.), further information is obtained in that the effect of guanine-quenching is about 55%. Considering that CSP8 displays 78% quenching which is induced by the conformational flexibility of single-stranded DNA, we can conclude that aggregation-induced self-quenching mechanism is one of the factors accounting for the low background fluorescence, whereas, the conformational flexibility of single-stranded DNA and guanine-quenching mechanism are the main

factors. All of them can be weakened by changing the molecular conformation to Watson-Crick duplexes *via* hybridization with complementary strands. In this way, the quenched fluorescence is expected to be restored.

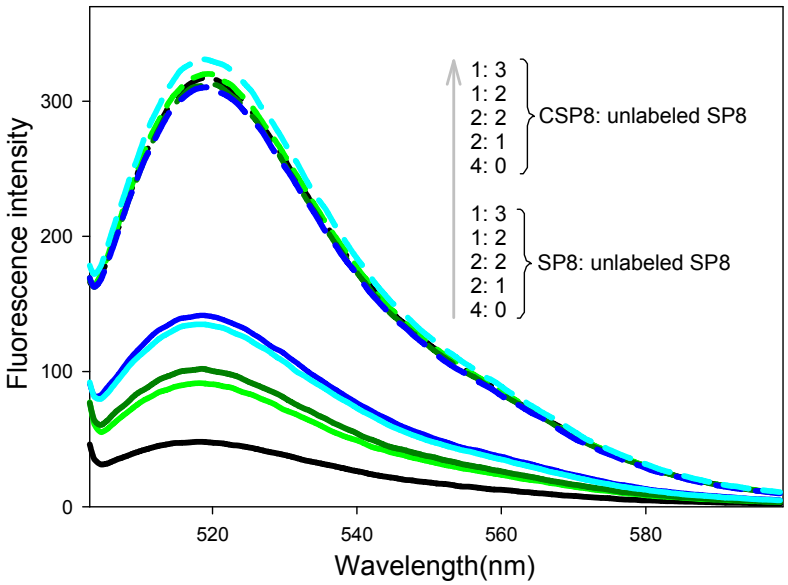

Fig. S3. Effect of unlabeled counterpart strand concentration on the fluorescence of signaling probes. The fluorescence spectra were collected for the reaction systems with 300 nM FAM-labeled SP8 or CSP8 at various labeled-unlabled ratios in buffer 1. Each spectrum presented is the average of three independent spectra.

2.4. Fluorescence Properties of IGQ Signaling Probe

To investigate whether the fluorescence change of signaling probe reflects the content of complementary strand or not, we measured the fluorescence spectra of SP8 upon hybridization to S1 at different concentrations. As shown in Fig. S4, the fluorescence peak at 516 nm firstly increases monotonically with increasing the concentration of S1 and finally reached a plateau. The Inset clearly depicts the dynamic relationship [$Y=0.8178+0.1365X-2.127\times10^{-4}X^2$] between the relative fluorescence intensity and the S1 concentration with a satisfactory regression coefficient (0.9997).

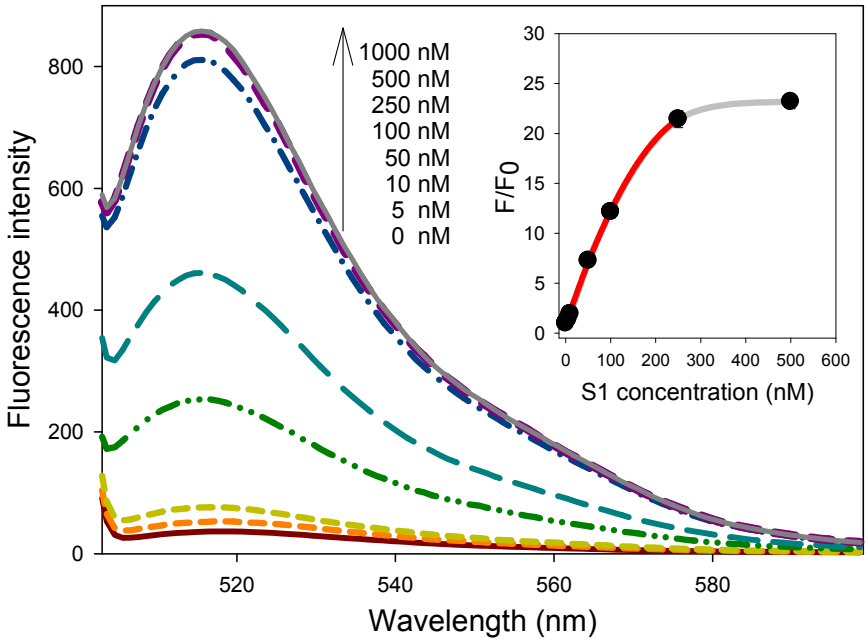

Fig. S4. Fluorescence intensity of G-rich signaling probe SP8, recorded at various concentrations of complementary stretching probe S1. As the concentration of S1 increases, the fluorescence intensity increases monotonously over a range of 5 nM to 250 nM. The regression equation with a correlation coefficient of 0.9997 is achieved, where Y and X represent the peak intensity and the S1 concentration, respectively. The error bars indicate the standard deviation of triplicate determinations for each concentration.

2.5. Application of IGQ Signaling Probe in IGQ-MB

In the initial stage of this work, we adopted electrophoresis analysis to obtain the direct evidence of the formation of IGQ signaling probe/MB1 complex. Comparing with CSP8 system, an additional lower mobility band can be observed when a half amount of MB1 was added in SP8, which is also slower and brighter than that in SP8 (Fig. S5), indicating that MB1 hybridizes with SP8 and the hybridized complex truly assemble into IGQ-structure. It is consistent with the reported.[S14] The different results between SP8 and CSP8 give further convincing evidence of expected IGQ-MB formation.

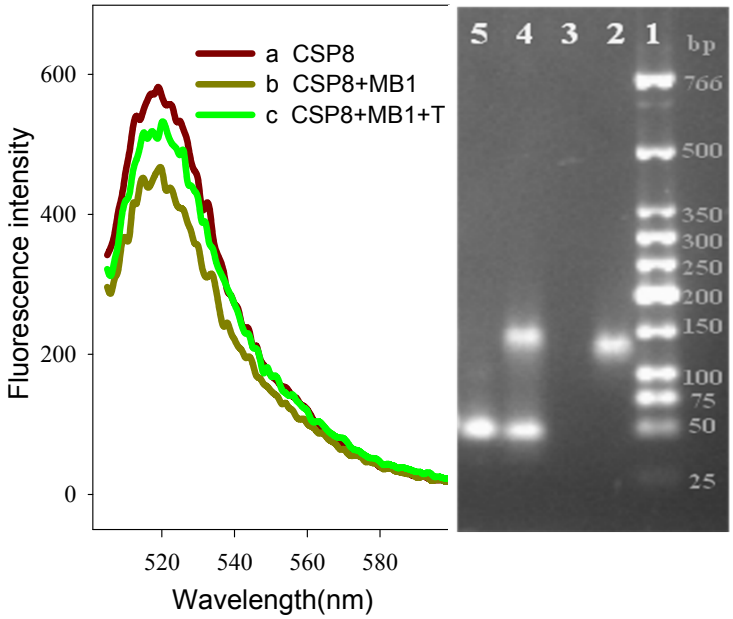

Fig. S5. Capability of CSP8 system to report target DNA: a) CSP8; b) CSP8/MB1; c) CSP8/MB1/target. The target concentration is 100 nM. **Right photo** is agarose gel electrophoresis image for different samples: lane 1) Low molecular weight DNA ladder; lane 2) SP8; lane 3) CSP8; lane 4) SP8/MB1 mixture; lane 5) CSP8/MB1 mixture.

Then, we explored the functioning principle of IGQ-MB system in fluorescence spectroscopy. As shown in Fig. S6B, the solution with SP8 alone is in a low signal state because of self-assembling into IGQ-structure. A slight fluorescence increase is displayed after addition of half dose of MB1. This result indicated the formation of the complex of IGQ-structure-based signaling probe/MB1 in which MB1 scarcely interfered with the intermolecular G-quadruplex and the signaling probes were kept in closed state. Upon addition of 100 nM target P53 gene, the fluorescence intensity of IGQ-MB system exhibited about 7-fold increase with the emission peak around 516nm, while, almost no increase was showed in control CSP8-system (shown in Fig. S5). Those clearly indicated that our proposed IGQ-MB strategy for detecting target DNA was feasible.

2.6. Important Role of the Shared Base in Segment 1

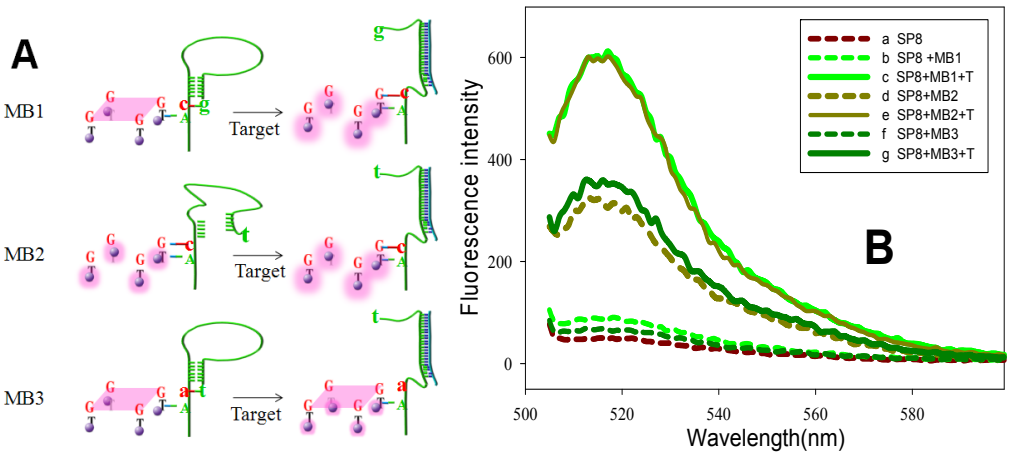

Fig. S6. (A) Structural change of SP8/MB1, SP8/MB2 and SP8/MB3 upon the addition of 100 nM target p53 gene. **(B)** Effect of MB's stem on the fluorescence response of IGQ-MB system. Comparing with MB1, MB2 is designed without hairpin structure by changing the segment2, MB3 is prepared with different stem bases via changing both segments. Therefore, in SP8/MB2 complex, the red "G-*c*" base pair can be obtained even in the absence of target DNA. In SP8/MB3 complex, there is no "G-*c*" base pair and the red G-quartet can not be changed regardless of target DNA.

The segment 1 (the shared c is involved) plays an important role in the design of IGQ-MB system. We can describe it as a bidirectional switch. When it pairs with the MB1's segment 2, switch turns to the side of MB1, the IGQ signaling probe keep its quenching behavior and the system is in closed state. When the shared base in segment 1 pairs with "G" base in nearby G-quartet of IGQ signaling probe, switch turns to the side of signaling probe, the quenching effect of signaling probe is weakened and the system is in open state, inducing the fluorescence restoration. Interestingly, the event of MB1-target DNA recognition reaction can control the switch and in turn controls the signal generation of signaling probe. That is to say, in our IGQ-MB system, MB1 acts as a recognizer, the segment 1 (the shared c is involved) is a switch, and the IGQ signaling probe is a reporter. Such division and

cooperation make the IGQ-MB function without any additional fluorophore or quencher modifications throughout the bone of MB. To validate the usefulness of the shared base in segment 1, two controlling molecular beacon probes, MB2 and MB3, were designed (shown in Fig. S6A). Without the shared c in the segment 1 of MB3, MB3 based IGQ-MB system should be in close state, even in the presence of target DNA. Thus, it expectantly displays not only low background fluorescence (line f in Fig. S6B) but also an obviously lower target induced signal (line g in Fig. S6B) *via* comparing with MB1 based system (line c in Fig. S6B). On the other hand, MB2 was designed without a hairpin structure by changing the segment2, the signaling probe/MB2 system should display a higher fluorescence intensity compared with MB1 even in the absence of target, because the shared c turn to the side of the signaling probe and make it be into open state. As expected, background fluorescence of the signaling probe/MB2 system increases by more than 3.7-fold (line d to line b in Fig. S6B). These experimental results offer convincing evidence to confirm the feasibility of the signaling mechanism described above.[S14] Nevertheless, both MB2 and MB3 exhibit detectable fluorescent signal upon target binding. This should be presumably attributed to the increase of molecular weight of signaling probe upon the hybridization of target and the resulting rigidity.

2.7. Optimization of Probe Ratio

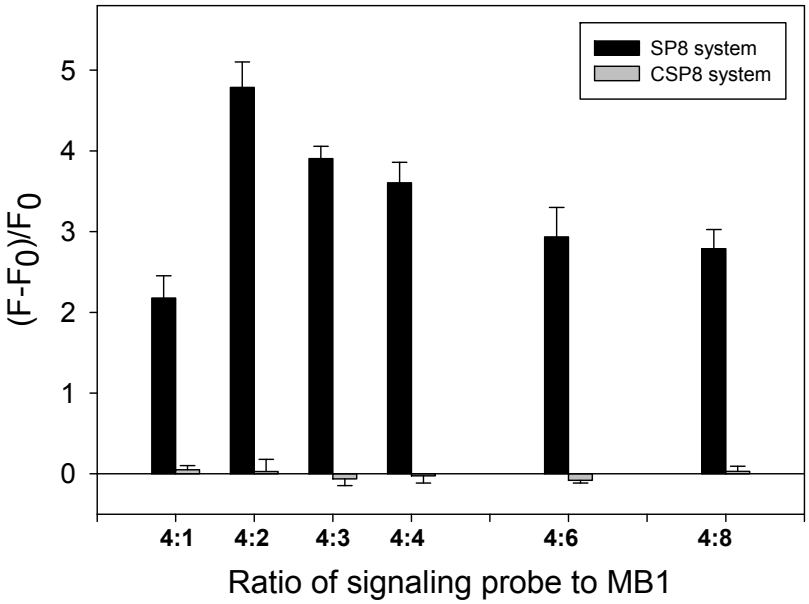

Fig. S7. The fluorescence response of target DNA was 100 nM at different ratios of signaling probe to MB1 in IGQ-MB system (blank) and CSP8-based control system (gray). In both systems (SP8 and CSP8), the concentration of MB1 was changed from 75, 150, 225, 300, 450, 600 to 750 nM, while the signaling probe was fixed at 300 nM. The corresponding ratios of signaling probe to MB1 were 4:1, 4:2, 4:3, 4:4, 4:6, 4:8 and 4:10, respectively. The error bars were obtained from at least three independent experiments.

In the present strategy, the binding of G-rich signaling probe (SP8) and MB1 plays a crucial role in constructing the IGQ-MB. Given a defined concentration (300 nM) of SP8, the molar ratio of SP8 to MB1 was investigated in order to achieve the optimal analytical performance. The fluorescence response of 100 nM target DNA increase as the ratio value increase (shown in Fig. S7). When the molar ratio reaches 4:2 (namely, 150 nM MB1 involved), the maximum fluorescence signal is achieved. Higher molar ratio brings a gradual decrease in fluorescence response. The result is consistent with the reported where 400 nM target DNA is used.[S14] Presumably, a large excess of MB1 disturbed self-assembling behavior of SP8s into IGQ-structure, which slowly increased background fluorescence. Therefore, an optimized ratio of 4:2 of signaling

probe to MB1 probe was used in the IGQ-MB system. The dosage of SP8 is more than MB probe, that is, one MB must pairs with at least two or four SP8s, indicating the achievement of our special binding model of IGQ-MB. In contrast, CSP8 system exhibits no obvious fluorescence change throughout this experiment, no matter which ratio is adopted.

2.8. Optimization of Ion and Temperature

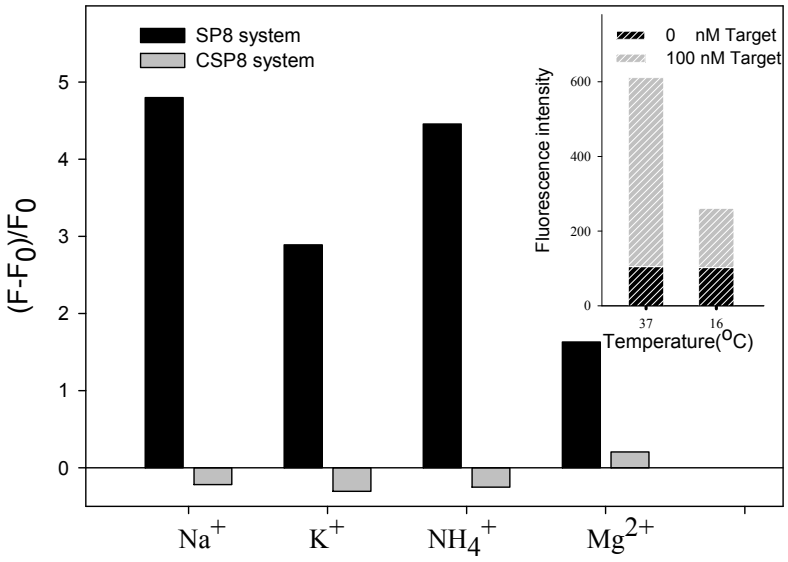

Fig. S8. The fluorescence responses of SP8-based IGQ-MB system (blank) and CSP8-based control system (gray) in Tris buffers (20 mM, pH 7.2) containing 100 mM monovalent cation (NaCl, or KCl, or NH_4Cl) or 50 mM $MgCl_2$). **Inset**: effect of reaction temperature on the fluorescence intensity of IGQ-MB system. The concentration of target DNA was 100 nM. The ratio of fluorescent probe to MB1 used was 4: 2.

Essentially, the detection performance of our IGQ-MB system is relative to the stability of G-quadruplex formed by SP8 and the hybridization efficiency between target DNA and MB1 recognizer. Thus, we investigated the fluorescence conduct in buffers with different metal cations and in different hybridizing temperature. In buffer containing Na^+, our IGQ-MB system displays a better fluorescence response (as

shown in Fig. S8). Additionally, the CD spectrum of SP8(shown in Fig. S11) also indicates that it forms intermolecular parallel G-quadruplex in Na^+ buffer. The fluorescence response to 100 nM target in 37 °C (inset of Fig. S8) was obviously better than that in 16 °C due to it promoted the hybridization of target to the loop of MB. Therefore, hybridization experiments were carried out at 37 °C in buffer containing 100 mM Na^+.

2.9. Analytical Performance of IGQ-MB

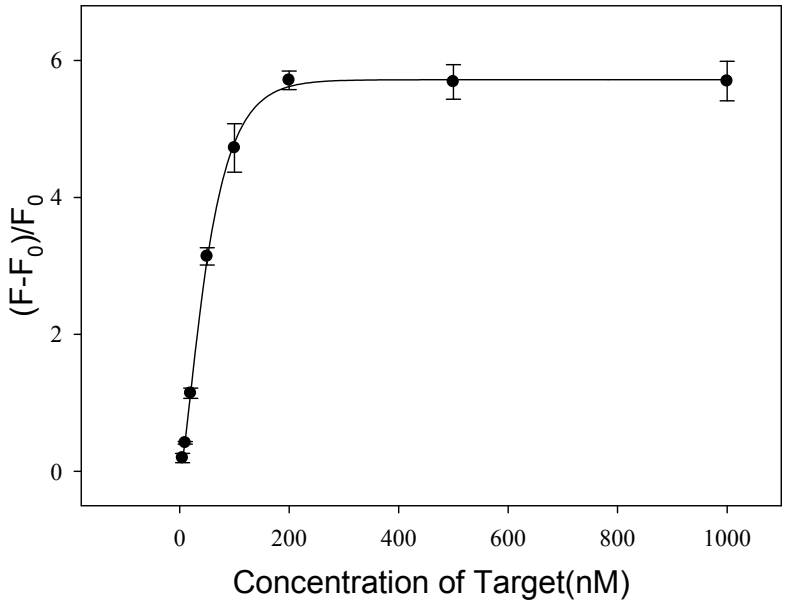

Fig. S9. The relationship between fluorescence signal and target p53 gene concentration. The ratio of SP8 to MB1 is 4: 2. The error bars represent the standard deviation of three measurements obtained at each target DNA concentration.

To demonstrate that the proposed IGQ-MB can be used for accurate quantification of target DNA, the fluorescence responses to P53 gene at various concentrations were evaluated. As shown in Fig. S9, the results represent a dynamic relationship between fluorescence response and the target concentration ranging from 5.00 to 200 nM with a calibration equation of $Y=5.718\times(1-\exp(-0.0225X))^{1.158}$. The satisfactory regression

coefficient is 0.9997. Meanwhile, the relative fluorescence responses to mutant target DNA with a nucleotide "A" substitutes for "G" in the wild region of p53 exon8 was measured, and about 64.0% of that upon the commentary target was obtained. The performance of this IGQ-MB system was further tested in Hela cancer cell lysate. A detectable fluorescence enhancement can be observed in sample containing as low as 5.00 nM target DNA (shown in Fig. S10). Moreover, the inset provides a good linear relationship between the fluorescence intensity (F) and target DNA concentration. The calibration equation is $Y=1303\times(1-\exp(-0.0276X))^{0.3997}$ with a correlation coefficient of 0.9928. The results revealed that the proposed IGQ-MB system showed promising properties for possible practical applications.

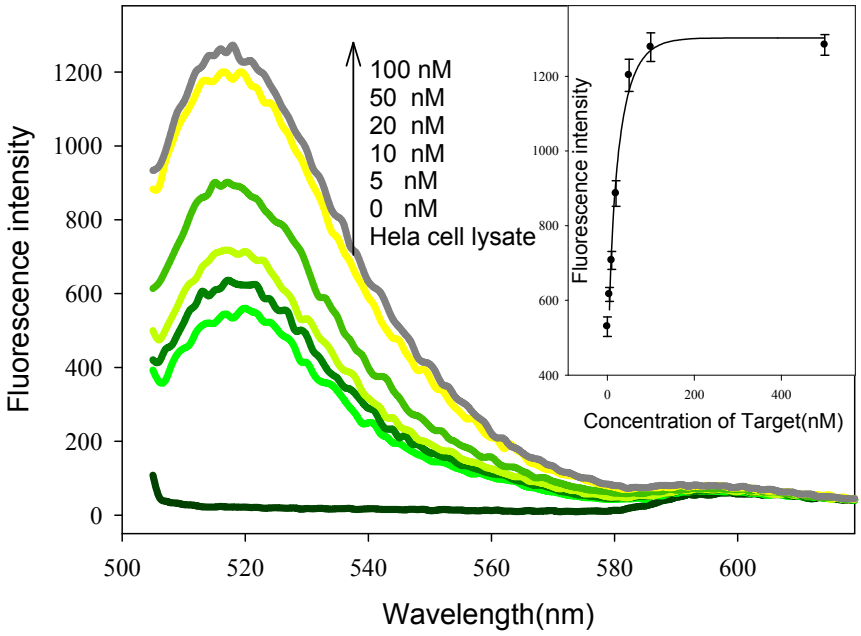

Fig. S10. Fluorescence spectra of IGQ-MB system Hela cell lysate upon different concentration of target p53 gene. **Inset** show the relationship between fluorescence signal and target p53 gene concentration. The ratio of SP8 to MB1 is 4: 2. The error bars represent the standard deviation of three measurements obtained at each target DNA concentration. The calibration equation is $Y=1303\times(1-\exp(-0.0276X))^{0.3997}$ with a correlation coefficient of 0.9928.

2.10. CD Spectral of Deferent G-rich Probe

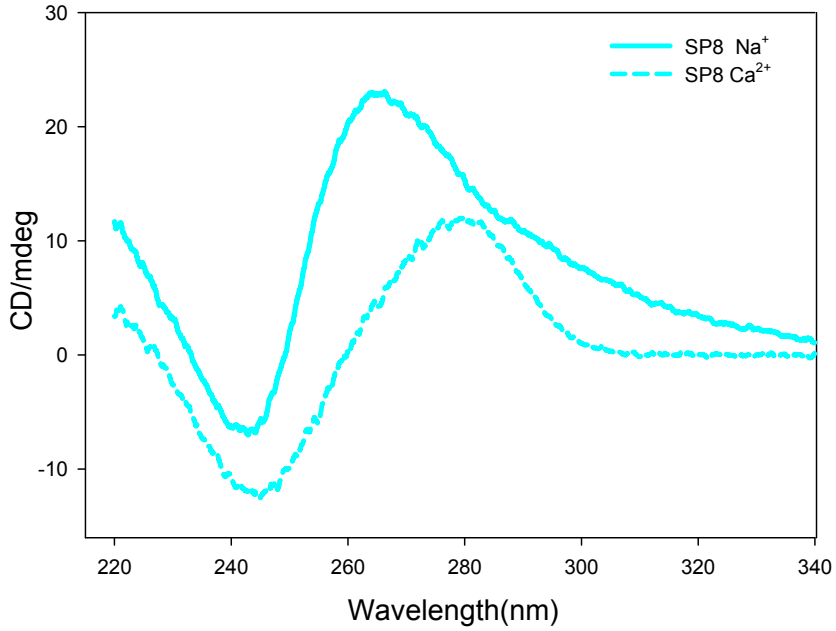

Fig. S11. CD spectra of 5 μM SP8 (solid line) and CSP8 (dot line) in the buffer containing 20 mM Tris (pH 7.2) 50 mM $CaCl_2$. All ODNs were unlabeled with FAMs.

As shown in Fig. S11, the SP8 displays the similar CD spectra of intermolecular parallel G-quadruplex structure with a positive signal at near 260 nm and a negative signal at 240 nm,[s14] which distinguish from spectral features of other single-stranded form of G-rich probes[s15] (a negative band at near 277 nm, a blue-shift of the peak and a decrease in the intensity of the trough at about 240 nm). It means that the signaling probe can assemble into the intermolecular parallel G-quadruplex structure regardless of the nature of metal ion dissolved in the buffer. The assembly behavior is consistent with the previous observation[s16].

3. Supplementary References

s1 R. S. Brody, K. G. Doherty and P. D. Zimmerman, *J. Biol. Chem*., 1986, **261**,7136.

s2 (*a*) Y. Yao, Q. Wang, Y. H. Hao and Z. Tan, *Nucleic Acids Res*, 2007, **35**, 2; (*b*) J. Tang, Z. Y. Kan, Y. Yao, Q. Wang, Y. H. Hao and Z. Tan, *Nucleic Acids Res.,* 2008, **36**,1200.

s3 S. Nakayama and H. O. Sintim, *J. Am. Chem. Soc.,* 2009, **131**, 10320.

s4 X. H. Cheng, X. J. Liu, T. Bing, Z. H. Cao and D. H. Shang-guan, *Biochemistry*.,2009, **48**, 7817.

s5 D. M. Kolpashchikov, *J. Am. Chem. Soc*., 2008, **130**, 2934.

s6 N. Borovok, N. Iram, D. Zikich, J. Ghabboun, G. I. Livshits, D. Porath, et al. *Nucleic Acids Res*., 2008, **36**, 5050.

s7 (*a*) E. Protozanova and R. B. Macgregor, *Biopolymers*., 2001, **58**, 355; (*b*) T. Y. Dai, S. P. Marotta and R. D. Sheardy, *Biochemistry*.,1995, **34**, 3655.

s8 E. Protozanova and R. B. Macgregor, *Biochemistry*. 1996, **35**, 16638.

s9 M. A. Keniry, *Biopolymers.,* 2001, **56**, 123.

s10 (*a*) O. Valdes-Aguilera and D. C. Necker, *Acc. Chem. Res.*, 1989, **22**, 171; (*b*) D. Avnir, D. Levy and R. Reisfeld, *J. Phys. Chem*., 1984, **88**, 5956.

s11 R. F. Chen and J. R. Knutson, *Anal. Biochem.,* 1988, **172**, 61.

s12 Y. J. Seo, H. Rhee and T. Joo, B. H. Kim, *J. Am. Chem. Soc.,* 2007, **129**, 5244.

s13 J. B. Randolph and A. S. Waggoner, *Nucleic Acids Res*., 1997, **25**, 2923.

s14 H. Zhou, Z. S. Wu, G. L. Shen and R. Q. Yu, *Biosensors. Bioelectron.,* 2012, DOI: 10.1016/j.bios.2012.08.028.

s15 (*a*) J. Y. Ju, C. C. Ruan, C. W. Fuller, A. N. Glazer and R. A. Mathies, *Proc. Natl. Acad. Sci. USA*, 1995, **92**, 4347; (*b*) Y. W. Wang, J. Y. Ju, B. A. Carpenter, J. M. Atherton, G. F. Sensabaugh and R. A. Mathies, *Anal. Chem.,* 1995, **67**, 1197.

s16 (*a*) D. M. Gray, *Biopolymers.*, 1974, **13**, 2087; (*b*) E. Protozanova and R. B. Macgregor, *Biophys J*., 1998, **75**, 982.